Recent studies to the impact of a ceramic breeder environment on the mechanical properties of EUROFER97 under operating conditions

E. Gaisina*, M. Duerrschnabel, J. Leys, R. Knitter, J. Aktaa, M. Walter

Karlsruhe Institute of Technology (KIT), Institute for Applied Materials, Hermann-von-Helmholtz-Platz 1, 76344 Eggenstein-Leopoldshafen, Germany

ARTICLE INFO

Keywords:
EUROFER
Ceramic breeder
Corrosion
Fatigue
Failure

ABSTRACT

The reduced activation ferritic-martensitic steel EUROFER is a prime candidate for fusion structural applications. In the advanced helium-cooled pebble bed blanket concept of DEMO, this steel is in direct contact with Li-ceramics pebbles and experiences cyclic thermomechanical loading under operating conditions. In this work, the effect of ceramic breeder environment on both the microstructure and particularly the fatigue properties of the RAFM steel was investigated. For this purpose, EUROFER samples were embedded in ceramic pebbles and annealed at 550 °C under a purge gas atmosphere for durations ranging 8–128 days. Microstructural studies show that annealing at the given conditions leads to the formation of a complex corrosion multilayer consisting of ferrite and iron oxide in an outer layer, as well as chromium oxide in both an intermediate and an inner layers. For annealing durations up to 32 days, the thickness of the oxide layer is continuously increasing. However, for more prolonged annealing, the thickness of the corrosion layer reaches saturation at about 20 µm. Similar to the growth behavior of the oxide layer, the strain-controlled LCF tests showed a remarkable reduction of the LCF lifetime with increasing in the annealing duration up to 32 days. However, beyond an annealing duration of 64 days, an additional decrease of lifetime is not observed. When performing additional experiments (annealing with ceramic pebbles in vacuum and annealing in purge gas without pebbles) it is found that corrosion is mainly caused by purge gas impurities, namely oxygen and water. Furthermore, the decrease in fatigue lifetime is related to the degradation of surface quality, causing an accelerated progress of damage. Finally, Charpy impact tests combined with carrier gas hot extraction investigations revealed that hydrogen embrittlement of the samples, annealed in a breeder environment containing 0.1 vol.% H_2, can be excluded.

1. Introduction

According to the helium-cooled pebble bed (HCPB) concept of DEMO, the reduced activation ferritic-martensitic (RAFM) steel EUROFER is used as a structural material, e.g. as pressure tubes in fuel-breeder pins [1–3]. These tubes are filled with a ceramic breeder material (Li_4SiO_4 / Li_2TiO_3 pebbles), which produces tritium under neutron irradiation that is used as fuel for the fusion reaction. The ceramic breeder pebbles are in direct contact with EUROFER pressure tube at higher temperatures up to 550 °C to avoid irradiation induced low-temperature hardening of steel [4]. At operating conditions, the contact triggers mutual diffusion of main constituent elements which lead to both the dissolution of ceramic breeder and corrosion of EUROFER [4–6]. Besides, the potential diffusion of lithium into EUROFER is of particular concern, since its transmutation under neutron irradiation can cause the formation of gasses (especially He that may form bubbles) and hence lead to a degradation of mechanical properties [7]. Furthermore, it needs to be considered that the steel pressure tubes, containing the ceramic pebble bed, are purged with a mixture of helium and 0.1 vol.% hydrogen to facilitate tritium release from the ceramic pebbles [1]. Hydrogen presents another potential risk because it diffuses relatively easily into metals, causing embrittlement. In addition, during the pulsed operation of the reactor, the EUROFER pressure tube will experience cyclic thermomechanical loading [8–11]. Thus, EUROFER needs to be operated under complex multifactorial conditions, including contact with ceramic pebbles, a purge gas atmosphere, strong neutron irradiation, elevated temperatures, and thermomechanical loads. Various experiments have been carried out to mimic such severe operating conditions. Microstructural changes in various RAFM steels under such conditions have already been studied in detail [4,5,12–15]. However, it remains unknown how the mechanical properties change, in particular fatigue properties, which are crucial in pulsed plasma conditions.

* Corresponding author.
E-mail address: elvina.gaisina@kit.edu (E. Gaisina).

This work continues the previous work aiming in evaluating the chemical compatibility between EUROFER and ceramic pebbles with respect to fatigue lifetime [16]. In this study, a new series of annealing experiments was carried out, including an extension of the annealing duration up to 128 days, mainly to investigate the growth behavior of the corrosion layer also under long-term conditions. Furthermore, to separate the effect of the ceramic pebbles from that of the purge gas on the corrosion behavior of the steel, two additional test series with customized annealing conditions were performed. Besides LCF tests on the differently treated samples, extensive microstructural investigations were used to determine the reason of the obtained differences in lifetime. Additionally, Charpy impact tests on both annealed and non-annealed samples were conducted to estimate a potential embrittlement of EUROFER by hydrogen uptake under breeder operating conditions. Finally, a novel TEM technique was used to determine the effect of Li uptake on the structural composition of the near-surface region of the steel.

2. Experimental details

Reduced activation ferritic-martensitic steel EUROFER97 batch 2 was used as a sample material. The steel has a composition of Fe-8.5Cr-1.1W-0.2Mn-0.15V-0.12Ta-0.1C (wt.%) and was received after heat treatment (960 °C for 1.5 h, oil quenching + 750 °C, 4 h, air cooling). For low cycle fatigue (LCF) investigations, sub-sized specimens exhibiting a nominal diameter of 2 mm and a gage length of 7.6 mm were prepared. To investigate the toughness behavior as a function of temperature, sub-sized Charpy-V specimens of KLST type with dimensions of 27 mm × 4 mm × 3 mm, a V-notch depth of 1 mm and a notch angle of 60° were manufactured. In addition, samples for metallographic studies with dimensions of 5 mm × 5 mm × 10 mm were cut and polished.

To mimic the working conditions of EUROFER pressure tubes in the HCPB design of DEMO, EUROFER samples were annealed in unconstrained contact with pebbles of lithium ceramics (70 mol.% Li_4SiO_4 and 30 mol.% Li_2TiO_3 [17,18]) at 550 °C in a purge gas flow atmosphere (ceramic breeder environment). The flow rate of purge gas, consisting of He and 0.1 vol.% H_2, was chosen to be 1200 ml/min at a pressure of 1200 mbar. The amount of gas impurities, particularly oxygen and water, was measured at the inlet and outlet of the furnace. A more detailed description of the test set-up is given in [19]. While LCF specimens, 9 per experiment, were annealed for 8, 16, 32, 64 and 128 days, respectively, Charpy samples were only annealed for 64 days.

To separate the effects of Li-ceramics and purge gas flow on the corrosion behavior of EUROFER, two additional annealing experiments were conducted. In the first additional experiment, 6 LCF specimens were annealed in contact with ceramic pebbles in vacuum for 64 days. In contrast, 6 other LCF specimens were annealed for 64 days in a flowing purge gas atmosphere without lithium ceramics pebbles.

Microstructural features of specimens were studied by X-ray diffraction (XRD), scanning electron microcopy (SEM) combined with energy dispersive X-ray spectroscopy (EDS). Additionally, electron-transparent lamellae prepared by focused ion beam (FIB) technique were examined using transmission electron microscopy (TEM).

Strain-controlled LCF tests were carried out in air at 550 °C, applying strain ranges of 0.6, 1, and 1.6%, respectively. The tests were performed using a strain rate of 3×10^{-3} s^{-1} and a fully-reversed triangular waveform ($R = -1$). Impact tests were conducted in a temperature range from −120 to −50 °C. Furthermore, carrier gas hot extraction was used to measure the amount of hydrogen in EUROFER samples.

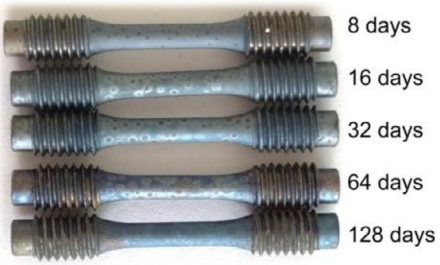

Fig. 1. LCF specimens of EUROFER after annealing for different durations together with ceramic pebbles in a purge gas atmosphere.

3. Results and discussion

3.1. Effect of annealing in a ceramic breeder environment on the microstructure of EUROFER

Fig. 1 presents the appearance of LCF specimens of EUROFER after annealing at 550 °C in contact with Li-ceramics pebbles in a purge gas flow atmosphere. The surface color of the specimens changed after annealing. After interaction for 8 days, black dots corresponding to the contact zones (imprints) of ceramic pebbles can be found. After annealing for 16–64 days, imprints are clearly visible as black dots surrounded by a brighter area. The imprints are barely visible after annealing for 128 days.

The change in the phase composition of the surface of EUROFER samples after annealing for different durations has been studied by X-ray diffraction analysis. The XRD patterns (Fig. 2) of the as-received EUROFER show only ferrite peaks (highlighted in green). After annealing for 8–32 days, in addition to ferrite peaks, strong peaks of FeO and Fe_3O_4/Fe_2O_3 appear. With an increase in the annealing time to 64 days, the intensity of the oxide peaks decreases. After annealing for 128 days, additional peaks were found in the XRD pattern, which were identified as $(Fe+Li)_3O_4$. Apparently, upon interaction for a long time, a sufficient amount of lithium diffuses from the lithium ceramic into the EUROFER surface, so that its amount exceeds the detection limit of XRD. This is in agreement with other works, in which lithium-containing oxide phases were also detected, but of different compositions, namely $Li_2Fe_3O_4$, $LiFe_5O_8$, $LiFeO_2$, and $LiCrO_2$ [4,13,20].

Fig. 3 presents results of surface analyses of EUROFER specimens after annealing in a ceramic breeder environment at 550 °C. After annealing with different durations, SEM micrographs and corresponding EDS maps were obtained from similar areas, depicting the contact zones with ceramic pebbles and their periphery (Fig. 3). EDS analysis shows that these contact zones after annealing for 8 days are composed of iron and chromium oxides. Most of the surface is covered with iron oxide. However, contact zones (steel-pebble) are dominated by chromium oxide. In addition, around imprints, hillocks of pure iron appear. With an increase in the annealing time to 16 days, the number of iron hillocks formed on the surface increases. After annealing for 32–128 days, the hillocks grow and merge, so that the surface is gradually covered by pure iron. Accordingly, as already reported in other works, the reduction of iron oxide by hydrogen is strongly increased with increasing interaction duration [13,20].

Both XRD and EDS analyses detected oxides on the EUROFER surface after annealing. The main sources of oxygen during annealing are the lithium ceramic itself and the purge gas, in which oxygen and water are present as impurities. The effect of purge gas is discussed in more detail in chapter 3.3. The XRD and EDS results are consistent in detecting that the amount of oxides on the surface decreases with increasing annealing duration. At the same

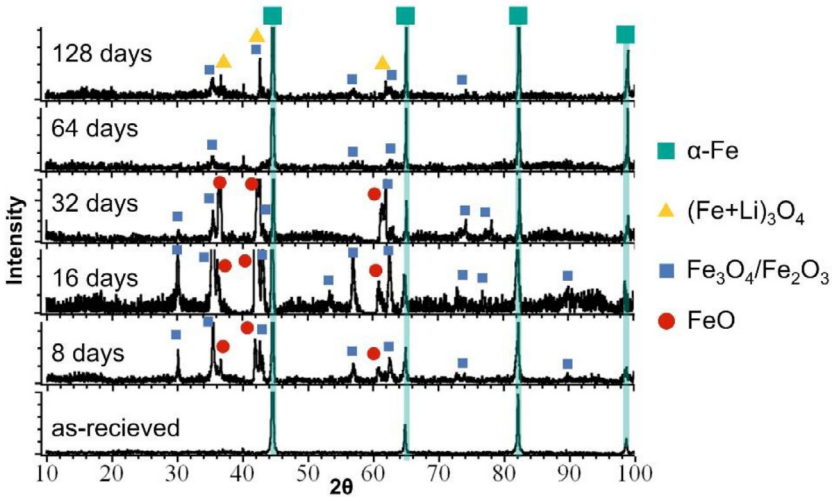

Fig. 2. X-ray diffraction patterns for as-received samples and after annealing for different durations with ceramic pebbles in a purge gas atmosphere.

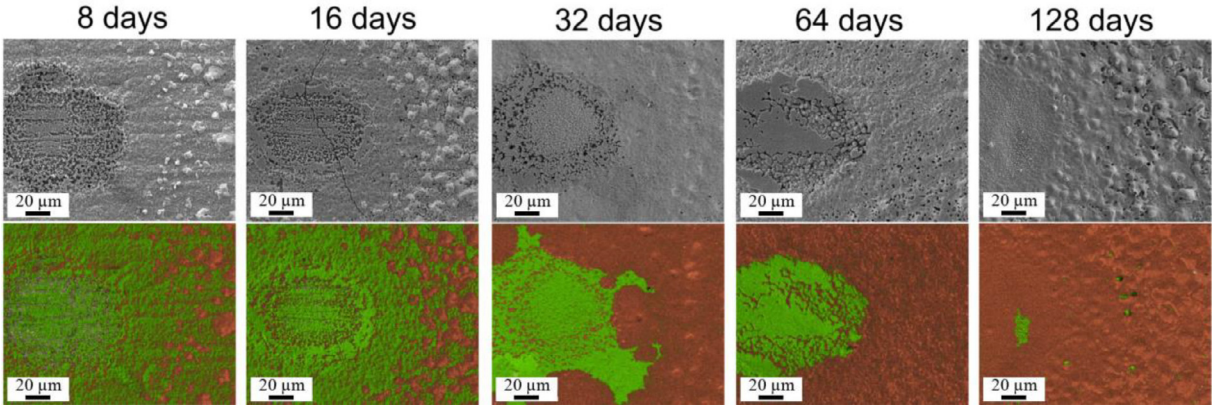

Fig. 3. Results of surface analyses of EUROFER samples after annealing with ceramic pebbles in a purge gas atmosphere for different durations. SEM micrographs are presented in the top row and corresponding EDS maps in the bottom row. On the EDS maps, oxides are highlighted in green and ferrite is highlighted in orange. (For interpretation of the references to colour in this figure legend, the reader is referred to the web version of this article.)

time, the reflection peaks of chromium oxide were not detected in XRD patterns, apparently due to their small volume fraction on the surface.

A cross-sectional SEM micrograph and elemental EDS mappings for a EUROFER sample annealed for 64 days are shown in Fig. 4. Three different corrosion layers can be distinguished. The outer corrosion layer with a higher Fe content (A in Fig. 4a) consists of two phases. The bright phase in the SEM micrograph (Fig. 4a) was identified as pure iron and the gray phase as Fe-rich oxide. Pure iron has pores and Fe-rich oxide is often cracked. The intermediate layer with a higher Cr content (B in Fig. 4a) consists of Cr-rich oxides. The inner corrosion layer (C in Fig. 4a) is adjacent to the EUROFER and contains Cr-rich oxides, formed at the lath boundaries of EUROFER. The total thickness of the corrosion layer after annealing for 64 days was measured to be about 13–18 μm. The same cross sections were also prepared for EUROFER samples annealed for all other durations. Fig. 5 presents the total thickness of corrosion layer of EUROFER versus annealing duration at 550 °C in the ceramic breeder environment. The diagram shows that the thickness of the corrosion layer gradually increases up to 64 days. With an increase in the duration of annealing to 128 days, the thickness of the corrosion layer does not change significantly and reaches about 12–20 μm.

Cross-sectional microstructural studies show the complexity of the corrosion layer formed during annealing of EUROFER in the ceramic breeder environment. The results are consistent with other works performed on EUROFER [4,13], F82H [20], and other RAFM steels [21]. Detailed corrosion studies of chromium-containing steel with gold markers left on the surface show that the corrosion layer with chromium oxide grows inward from the gold markers, and iron oxide grows towards the outside of the former surface of the steel [22]. Thus, iron atoms diffuse through the chromium oxide layer to the surface where they form iron oxide.

As already mentioned, if lithium atoms diffuse into EUROFER due to long-term contact with ceramic pebbles at elevated temperatures, then during neutron irradiation in the fusion reactor, these lithium atoms can transmute forming gasses that would deteriorate the mechanical properties of the steel. In order to study the result of lithium penetration more detailed, several lamellae from the corrosion layers were prepared by FIB for TEM study. For this purpose, a cross-section of a EUROFER sample was used after annealing for 64 days in contact with ceramic pebbles in a purge gas atmosphere. Fig. 6 shows a lamella that was lifted out from the outer corrosion layer (layer A in Fig. 4a). Ferrite and $LiFeO_2$ oxide were identified by electron diffraction analysis. Some pores were found in the ferrite phase. Lithium was not found in the ferrite phase, apparently due to its insolubility in iron [23]. Another lamella was lifted out across the whole corrosion layer (Fig. 7a). This lamella represents all three corrosion layers that have been identified in Fig. 7a in analogy to Fig. 4a. The intermediate layer, consisting of fine-grained particles, was studied in more detail (Fig. 7b). A crack was found at the boundary between the interme-

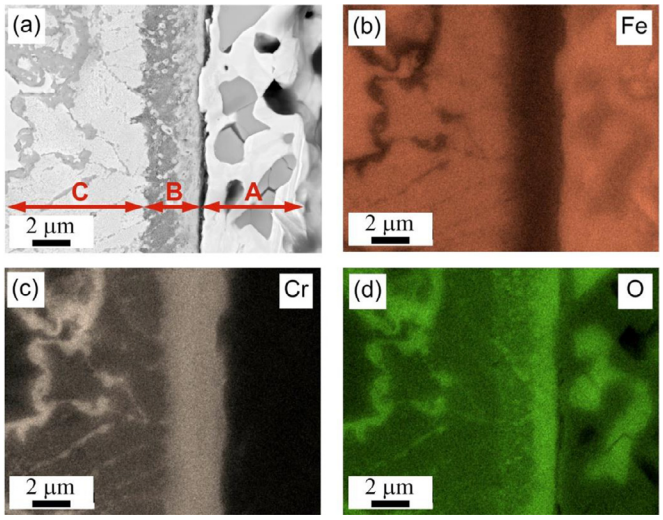

Fig. 4. (a) Microstructure and (b-d) corresponding elemental EDS maps of a cross section of EUROFER sample annealed with ceramic pebbles in a purge gas atmosphere: (b) iron, (c) chromium, (d) oxygen. In (a), three different corrosion layers can be distinguished: outer A with a higher Fe content, intermediate B with higher Cr content, and inner C adjacent to EUROFER.

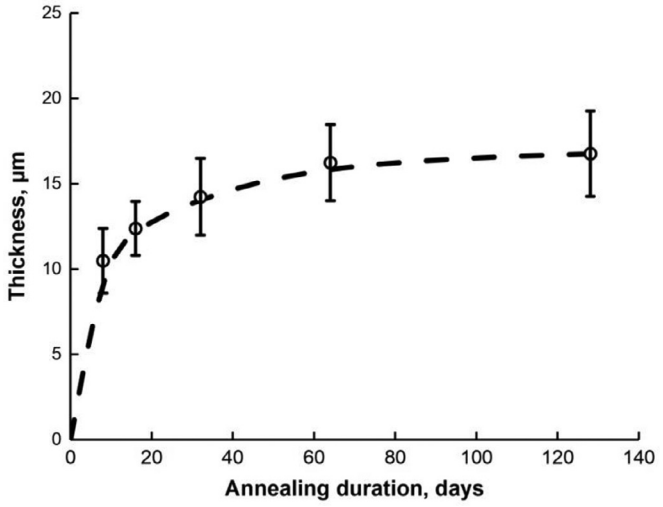

Fig. 5. The total corrosion thickness of EUROFER depending on the duration of annealing with ceramic pebbles in a purge gas atmosphere.

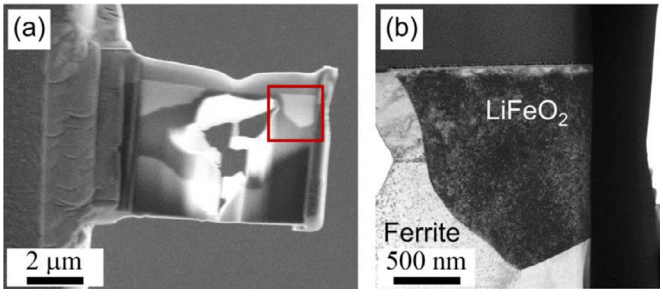

Fig. 6. (a) General view of the TEM lamella lifted out from the outer corrosion layer of EUROFER annealed for 64 days, and (b) TEM image of the area indicated by the red square in (a). (For interpretation of the references to colour in this figure legend, the reader is referred to the web version of this article.)

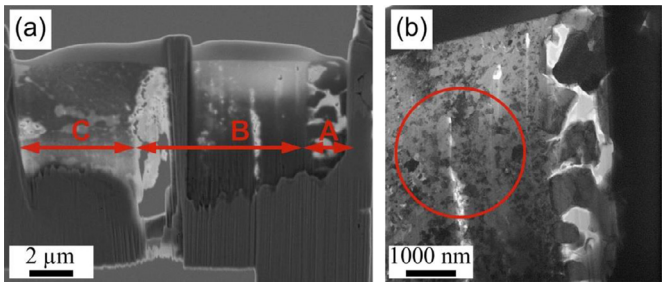

Fig. 7. (a) General view of the TEM lamella lifted out across three different corrosion layers (A, B, and C) of EUROFER annealed for 64 days, and (b) TEM image of the right window in (a). A red circle on (b) indicates an area that was identified as $Li_2Fe_{3.2}Cr_{6.8}O_{16}$ by diffraction analysis. (For interpretation of the references to colour in this figure legend, the reader is referred to the web version of this article.)

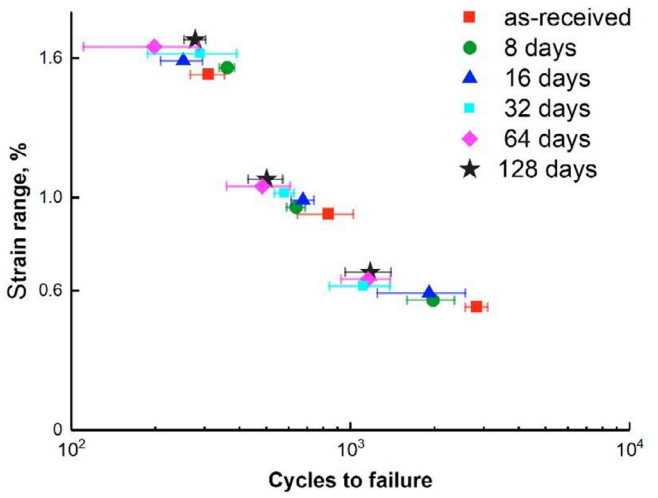

Fig. 8. Results of the LCF tests of EUROFER specimens annealed for different durations with ceramic pebbles in a purge gas atmosphere. The specimens were tested at 550 °C at three different total strain ranges of 0.6, 1, and 1.6%. Vertical offset within a strain range is used to avoid data overlap.

diate and inner corrosion layers, which is also often observed on metallographic cross-sections. The TEM diffraction analysis of the intermediate corrosion layer determined its crystal structure as of $Li_2Fe_{3.2}Cr_{6.8}O_{16}$ type. Crystal structures of non-lithium containing oxides did not fully explain the diffraction pattern. Thus, the TEM study revealed the diffusion of lithium into the corrosion layers of EUROFER after annealing in ceramic breeder environment. A separate work will be devoted to a more detailed analysis of lithium-containing phases in the corrosion layer of EUROFER.

3.2. Effect of annealing in a ceramic breeder environment on the fatigue life of EUROFER

The results of LCF tests on the as-received and annealed samples are presented in Fig. 8. They generally confirm and extend the results obtained in the previous work [16]. The diagram shows a remarkable reduction of the LCF lifetime with an increase in annealing duration, particularly at total strain ranges of 0.6 and 1%. At the strain range of 0.6%, the reduction in the lifetime is approximately 50% for an annealing duration of 32–128 days. When plotting the number of cycles to failure versus annealing duration (Fig. 9), it can be seen quite well that the strongest decrease in lifetime is found for samples annealed up to 32 days. However, the subsequent increase in the annealing duration does not have an additional significant effect on the fatigue life. Taking into account the results depicted in Fig. 5, this new series of tests clearly shows

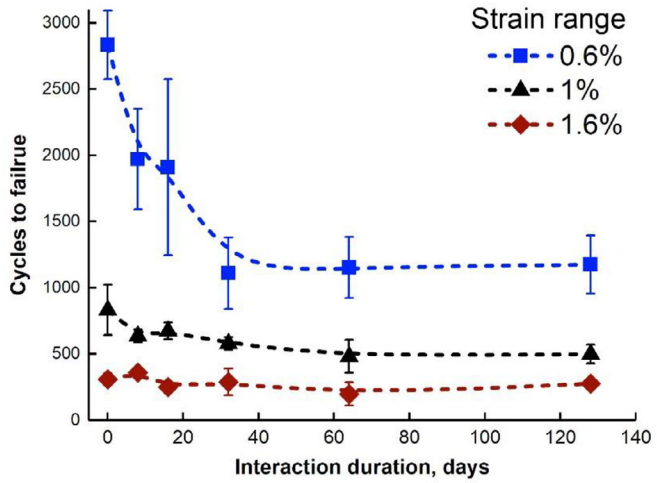

Fig. 9. Number of cycles to failure plotted versus annealing duration for three different total strain ranges of 0.6, 1, and 1.6%.

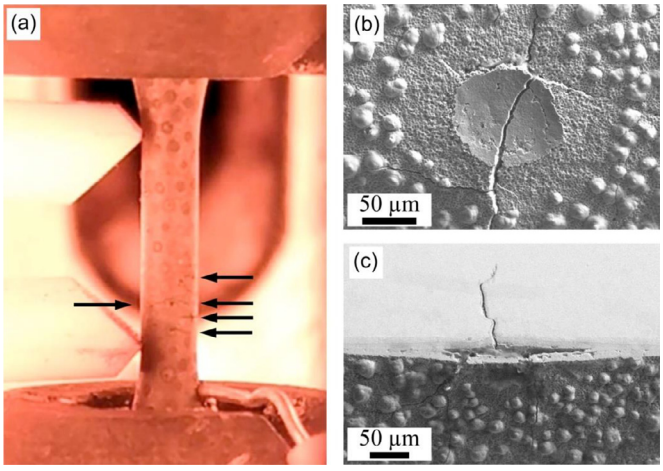

Fig. 10. (a) Cracking of the EUROFER specimens close to the imprints of ceramic pebbles: (a) specimen in the tension phase of the LCF test, (b) specimen surface after testing, (c) cross-section of imprints after testing. In (a), black arrows indicate the cracks propagating from the imprints.

that when reaching a certain oxide layer thickness leads to a passivation of the steel surface and, therefore, to a stop of the materials degradation. Consequently, the decrease in lifetime is also limited – but to a fairly low level, especially for low cyclic loads.

The dramatic effect on fatigue lifetime is unambiguously the result of corrosion caused by annealing the specimens in contact with ceramic pebbles in a purge gas atmosphere. The surface structure plays an important role, since under cyclic loading, both the formation and growth behavior of surface micro-cracks are significantly affecting the lifetime of a component. In this case, the degradation of fatigue properties is obviously related to:

- already existing surface micro-cracks (see Fig. 3 upper row picture 2 – 16 days), probably formed during cooling down the samples when taking them out of the furnace (appearance of residual stresses, caused by different thermal expansion coefficients of EUROFER and chrome oxides);
- an accelerated formation of additional surface micro-cracks, based on local stress concentrations caused by the strong increase of surface roughness (particularly imprints need to be seen as notches – see Fig. 10);
- an accelerated growth of micro-cracks through the brittle oxide layers on the surface (see Fig. 10).

Fig. 11. LCF specimens of EUROFER for additional experiments: (a) after annealing with ceramic pebbles in vacuum for 64 days, (b) after annealing in a purge gas atmosphere for 64 days.

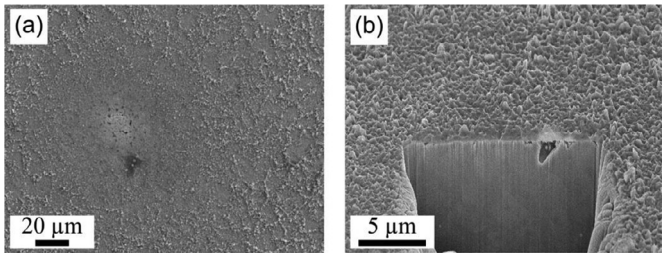

Fig. 12. EUROFER sample after annealing with ceramic pebbles in vacuum for 64 days: (a) SEM of the surface close to the ceramic pebble imprint and (b) FIB cut into a sample showing a very thin corrosion layer.

3.3. Additional annealing experiments

Fig. 11 presents the appearance of LCF specimens of EUROFER after additional annealing experiments. In the first experiment, the specimens were annealed at 550 °C for 64 days in contact with lithium ceramic pebbles in vacuum. In contrast to the main experiment, the imprints of lithium ceramics in this case are barely noticeable, and the sample has a brownish color (Fig. 11a). In the second experiment, the specimens were annealed at 550 °C for 64 days in a purge gas atmosphere without ceramic pebbles. The specimens have a bluish color (Fig. 11b), comparable to the specimens from the main experiment (Fig. 1).

Fig. 12 presents the microstructure of EUROFER specimens after annealing at 550 °C in contact with Li-ceramic pebbles in vacuum for 64 days. The imprint of ceramic pebbles is barely visible and the surface is covered by tiny needles of iron and chromium oxides, which was confirmed by EDS (not shown). The thickness of the corrosion layer is so small that it was only revealed in cross-sections during FIB cutting (Fig. 12b). The thickness of the layer turned out to be 0.45–0.85 µm, which is significantly smaller than the thickness of layers from samples annealed under breeder environment conditions (13–18 µm). Accordingly, it is found that the impact of the pebbles on the corrosion behavior of the steel under breeder operating conditions is more or less negligible. Similar results were reported in [15].

Fig. 13 shows results of surface analyses of EUROFER specimen after annealing at 550 °C in a purge gas flow atmosphere for 64 days. The surface of the sample is covered with pure iron hillocks. In-between, iron and chromium oxides are found. The corrosion layer resembles the surface of the sample in the main experiment in the periphery of contact zones with ceramic pebbles (Fig. 3). Cross-sectional microstructural studies were used to measure the thickness of the corrosion layer. It is found to be 13–17 µm, so comparable to the thickness of layers from samples aged under breeder environment conditions. Taking into account the result obtained on samples annealed in vacuum, it becomes clear that despite their small volume fractions, purge gas impurities, namely

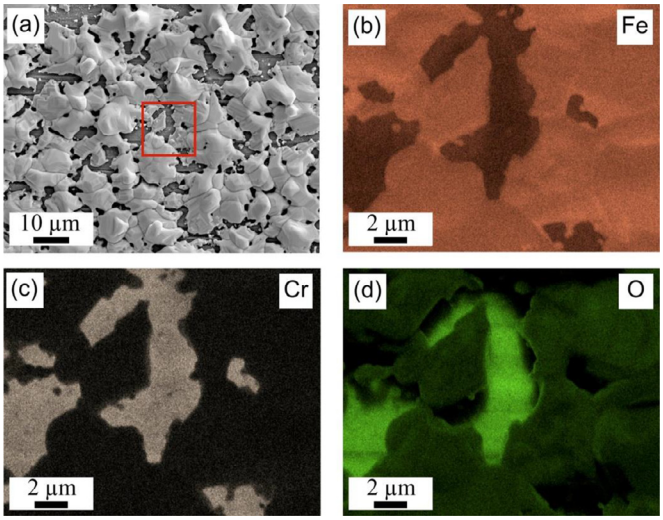

Fig. 13. (a) Results of surface analyses of EUROFER samples after annealing in a purge gas atmosphere for 64 days: (a) SEM micrographs and (b-c) elemental EDS maps: (b) iron, (c) chromium, (d) oxygen. The EDS maps correspond to the indicated red square in (a). (For interpretation of the references to colour in this figure legend, the reader is referred to the web version of this article.)

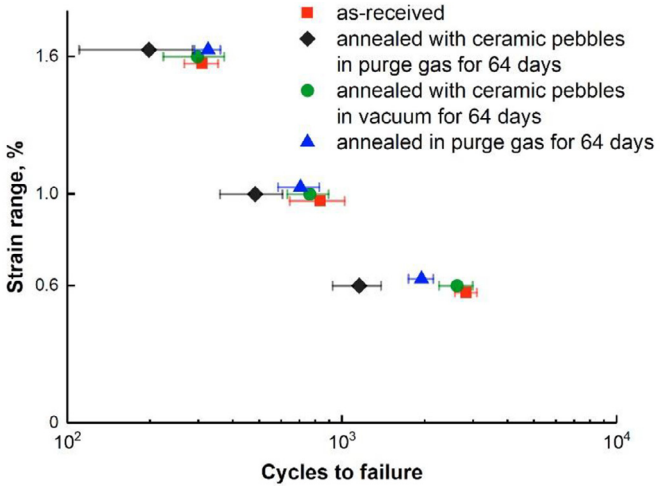

Fig. 14. Results of the LCF tests of EUROFER specimens in as-received and annealed conditions. The specimens were tested at 550 °C at three different total strain ranges of 0.6, 1, and 1.6%. Vertical offset within a strain range is used to avoid data overlap.

oxygen and water (0.18 and 0.0053 vol.% of oxygen and water, respectively, at the inlet of the furnace), are mainly responsible for the chemical attack on the steel surface.

The LCF test results obtained from tests performed on the additional treated samples are plotted together with the results obtained from tests on both as-received specimens and specimens annealed under breeder conditions (Fig. 14). The diagram shows that compared to the as-received state, annealing with ceramic pebbles in vacuum has no significant effect on the LCF lifetime. In contrast, annealing in a purge gas flow atmosphere significantly reduces the LCF lifetime, but not as much as annealing in both pebbles and purge gas. This is obviously related to the absence of imprints, mainly resulting in a delayed formation of micro-cracks.

Generally, the corrosion of EUROFER subjected to a breeder environment could be significantly reduced by removing purge gas impurities (oxygen and water). However, in the new design of the HCPB concept, it is proposed to use water, since it facilitates the tritium transport [24]. This implies the development of protective coatings on EUROFER surface that not only solve the problem of corrosion and deterioration of mechanical properties, but also prevent tritium permeation and lithium penetration into the steel. Recently, several attractive protective coatings have been developed [20,25–27], but their compatibility with EUROFER during cyclic loading needs to be verified. In addition, the design of the HCPB blanket could be changed so that EUROFER does not exhibit a contact with ceramic pebbles as structural material.

3.4. Effect of a ceramic breeder environment on impact properties of EUROFER

Since EUROFER in the HCPB concept is operated in a purge gas atmosphere containing 0.1 vol.% of hydrogen, it was assumed that hydrogen atoms could diffuse into the material and cause an additional embrittlement [16]. To detect a possible hydrogen embrittlement, Charpy impact tests on EUROFER specimens, subjected to a ceramic breeder environment for 64 days, were performed. For comparison, as-received specimens were tested, as well as speci-

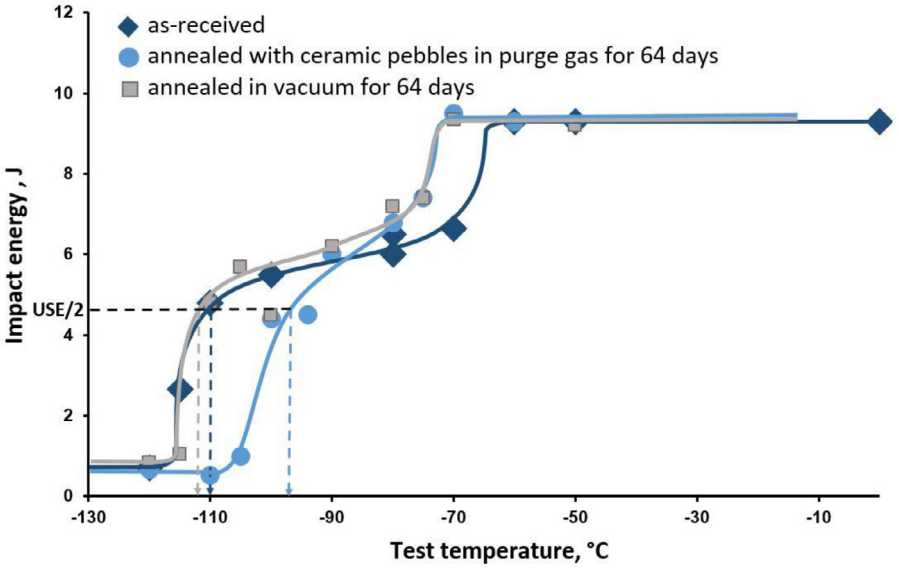

Fig. 15. Charpy impact energy versus test temperature curves for as-received and annealed EUROFER.

mens annealed in vacuum (without ceramic pebbles) for 64 days. The experiments were carried out at temperatures ranging from −120 to −50 °C.

Fig. 15 presents the results of Charpy impact tests. In general, the results of the impact tests for all specimens are similar. The ductile to brittle transition temperature (DBTT), determined at half upper shelf energy (USE/2), is found to be −110, −97, and −113°C for the as-received, annealed in ceramic breeder environment, and annealed in vacuum states, respectively. Taking into account the general progress of the different curves one may assume that the slight differences are mainly related to slight differences in crack initiation. When comparing the upper shelf energy (USE) of the annealed samples with the one of the as-received samples, one can practically see no difference. Accordingly, a significant embrittlement of the samples annealed in a breeder environment can be excluded.

Subsequently performed carrier gas hot extraction investigations confirmed this result. While the as-received EUROFER shows an amount of hydrogen lower than the precision of measurement (<0.23 ppm), a sample annealed in a ceramic breeder environment reveals an amount of hydrogen of 6.7 ± 1.0 ppm. When removing the entire corrosion layer by grinding, the amount of hydrogen turned out to be much less and reaches 2.6 ± 0.3 ppm. Accordingly, most of the hydrogen is concentrated in the corrosion layer close to the surface and only a very small amount of hydrogen diffuses into the material.

4. Conclusions

Within the frame of this work, the effect of annealing in direct contact with Li-ceramic pebbles in a purge gas atmosphere on the microstructure and mechanical properties of EUROFER was investigated. Microstructural studies reveal the complexity of the corrosion layer formed during annealing. The outer corrosion layer is composed of ferrite and Fe-rich oxide. This oxide can also contain lithium as shown by XRD and TEM. The intermediate corrosion layer is formed by Cr-rich oxides, which can also contain iron and lithium. In the inner corrosion layer adjacent to EUROFER, chromium oxides are often located along the lath boundaries of the steel. The total thickness of the corrosion layer reaches saturation after annealing beyond 32 days and is measured to be 12–20 µm. In contact zones with ceramic pebbles, cracks are often found both after fatigue tests and before them.

The strain-controlled LCF tests performed at 550 °C show a remarkable reduction of the LCF lifetime with an increase in the annealing duration. At total strain range of 0.6%, the reduction in the lifetime compared to as-received specimens is approximately 50% for an annealing duration of 64–128 days. The LCF lifetime decreases most rapidly for the annealing duration of 8–32 days, while it appears to saturate when the annealing time is increased to 128 days.

To separate the effect of Li-ceramic pebbles from that of the flowing purge gas on the corrosion behavior of the steel, two additional annealing experiments were performed with deviating conditions. It turned out that annealing in contact with ceramic pebbles in vacuum practically does not lead to corrosion of EUROFER and thus, does not reduce the LCF lifetime. In contrast, annealing in a purge gas flow atmosphere leads to significant corrosion due to impurities, namely oxygen and water, and significantly shortens the LCF lifetime, but not as much as annealing at breeder conditions.

Charpy impact tests and carrier gas hot extraction tests confirmed that a possible embrittlement of EUROFER by hydrogen uptake during annealing can be excluded.

The results obtained indicate the need to protect the EUROFER surface from corrosion during its operation in the HCPB blanket concept so that the fatigue properties of the structural steel do not deteriorate in ceramic breeder environment.

Declaration of Competing Interest

The authors declare that they have no known competing financial interests or personal relationships that could have appeared to influence the work reported in this paper.

CRediT authorship contribution statement

E. Gaisina: Writing – review & editing, Methodology, Investigation, Visualization. **M. Duerrschnabel:** Methodology, Investigation, Writing – review & editing. **J. Leys:** Methodology, Writing – review & editing. **R. Knitter:** Methodology, Writing – review & editing. **J. Aktaa:** Supervision, Conceptualization, Methodology, Writing – review & editing. **M. Walter:** Supervision, Methodology, Investigation, Writing – review & editing.

Acknowledgements

This work has been carried out within the framework of the EUROfusion Consortium and has received funding from the Euratom research and training program 2014–2018 and 2019–2020 under grant agreement No 633053. The views and opinions expressed herein do not necessarily reflect those of the European Commission. We thank Dr. Klaus Seemann for XRD analysis, Dr. Ramil Gaisin for FIB lamellae preparation, Dr. Thomas Bergfeldt for carrier gas hot extraction investigations.

References

[1] F.A. Hernández, P. Pereslavtsev, G. Zhou, B. Kiss, Q. Kang, H. Neuberger, V. Chakin, R. Gaisin, P. Vladimirov, L.V. Boccaccini, G.A. Spagnuolo, S. D'Amico, I. Moscato, Advancements in the helium-cooled pebble bed breeding blanket for the EU DEMO: holistic design approach and lessons learned, Fusion Sci. Technol. 75 (2019) 352–364, doi:10.1080/15361055.2019.1607695.

[2] M. Gorley, G. Aiello, J. Henry, T. Nozawa, G. Pintsuk, M. Rieth, H. Tanigawa, DEMO structural materials qualification and development, Fusion Eng. Des. 170 (2021) 112513, doi:10.1016/j.fusengdes.2021.112513.

[3] R. Lindau, A. Möslang, M. Rieth, M. Klimiankou, E. Materna-Morris, A. Alamo, A.-A.F. Tavassoli, C. Cayron, A.-.M. Lancha, P. Fernandez, N. Baluc, R. Schäublin, E. Diegele, G. Filacchioni, J.W. Rensman, B.v.d. Schaaf, E. Lucon, W. Dietz, Present development status of EUROFER and ODS-EUROFER for application in blanket concepts, Fusion Eng. Des. 75-79 (2005) 989–996, doi:10.1016/j.fusengdes.2005.06.186.

[4] K. Mukai, F. Sanchez, R. Knitter, Chemical compatibility study between ceramic breeder and EUROFER97 steel for HCPB-DEMO blanket, J. Nucl. Mater. 488 (2017) 196–203, doi:10.1016/j.jnucmat.2017.03.018.

[5] T. Hernández, P. Fernández, Effect of the environment on the corrosion of EUROFER97 by solid lithium breeders, J. Nucl. Mater. 447 (2014) 160–165, doi:10.1016/j.jnucmat.2013.12.026.

[6] L.C. Alves, E. Alves, M.R. da Silva, A. Paúl, A. La Barbera, Li ceramic pebbles chemical compatibility with EUROFER samples in fusion relevant conditions, J. Nucl. Mater. 329-333 (2004) 1295–1299, doi:10.1016/j.jnucmat.2004.04.227.

[7] M.J. Demkowicz, A. Misra, A. Caro, The role of interface structure in controlling high helium concentrations, Curr. Opin. Solid State Mater. Sci. 16 (2012) 101–108, doi:10.1016/j.cossms.2011.10.003.

[8] K. Mariappan, V. Shankar, R. Sandhya, G.V. Prasad Reddy, M.D. Mathew, Dynamic strain aging behavior of modified 9Cr–1Mo and reduced activation ferritic martensitic steels under low cycle fatigue, J. Nucl. Mater. 435 (2013) 207–213, doi:10.1016/j.jnucmat.2012.12.049.

[9] A. Abou-Sena, B. Löbbecke, A. von der Weth, R. Knitter, Effect of post welding heat treatment of the HCPB TBM on EUROFER and lithium orthosilicate pebbles, Fusion Eng. Des. 86 (2011) 2254–2257, doi:10.1016/j.fusengdes.2011.03.038.

[10] K. Zhang, M. Walter, J. Aktaa, Ratcheting and fatigue behavior of EUROFER97 at high temperature, part 1: experiment, Fusion Eng. Des. 150 (2020) 111407, doi:10.1016/j.fusengdes.2019.111407.

[11] P. Marmy, T. Kruml, Low cycle fatigue of EUROFER 97, J. Nucl. Mater. 377 (2008) 52–58, doi:10.1016/j.jnucmat.2008.02.054.

[12] K. Mukai, M. Gonzalez, R. Knitter, Effect of moisture in sweep gas on chemical compatibility between ceramic breeder and EUROFER97, Fusion Eng. Des. 125 (2017) 154–159, doi:10.1016/j.fusengdes.2017.10.001.

[13] K. Mukai, F. Sanchez, T. Hoshino, R. Knitter, Corrosion characteristics of reduced activation ferritic-martensitic steel EUROFER by Li2TiO3 with excess Li, Nucl. Mater. Energy 15 (2018) 190–194, doi:10.1016/j.nme.2018.04.010.

[14] T. Hernández, M.C. Gázquez, F.J. Sánchez, M. Malo, Corrosion mechanisms of EUROFER produced by lithium ceramics under fusion relevant conditions, Nucl. Mater. Energy 15 (2018) 110–114, doi:10.1016/j.nme.2018.03.005.
[15] T. Hernández, P. Fernández, R. Vila, Corrosion susceptibility of EUROFER97 in lithium ceramics breeders, J. Nucl. Mater. 446 (2014) 117–123, doi:10.1016/j.jnucmat.2013.11.047.
[16] J. Aktaa, M. Walter, E. Gaisina, M.H.H. Kolb, R. Knitter, Assessment of the chemical compatibility between EUROFER and ceramic breeder with respect to fatigue lifetime, Fusion Eng. Des. 157 (2020) 111732, doi:10.1016/j.fusengdes.2020.111732.
[17] R. Knitter, M.H.H. Kolb, U. Kaufmann, A.A. Goraieb, Fabrication of modified lithium orthosilicate pebbles by addition of titania, J. Nucl. Mater. 442 (2013) S433–S436, doi:10.1016/j.jnucmat.2012.10.034.
[18] O. Leys, J.M. Leys, R. Knitter, Current status and future perspectives of EU ceramic breeder development, Fusion Eng. Des. 164 (2021) 112171, doi:10.1016/j.fusengdes.2020.112171.
[19] J.M. Heuser, M.H.H. Kolb, T. Bergfeldt, R. Knitter, Long-term thermal stability of two-phased lithium orthosilicate/metatitanate ceramics, J. Nucl. Mater. 507 (2018) 396–402, doi:10.1016/j.jnucmat.2018.05.010.
[20] T. Chikada, M.H.H. Kolb, H. Fujita, K. Nakamura, K. Kimura, M. Rasinski, Y. Hishinuma, K. Mukai, R. Knitter, Compatibility of tritium permeation barrier coatings with ceramic breeder pebbles, Corros. Sci. 182 (2021) 109288, doi:10.1016/j.corsci.2021.109288.
[21] S. Sonak, U. Jain, R. Haldar, S. Kumar, Chemical compatibility study of lithium titanate with Indian reduced activation ferritic martensitic steel, Fusion Eng. Des. 100 (2015) 507–512, doi:10.1016/j.fusengdes.2015.07.026.
[22] Vicente Braz Trindade, Rodrigo Borin, Behzad Zandi Hanjari, Songlang Yang, Ulrich Krupp, Hans-Jürgen Christ, High-temperature oxidation of pure Fe and the ferritic steel 2.25Cr1Mo, Mater. Res. 8 (4) (2005).
[23] L. Cornish, Y. Eichhammer, D. Pavlyuchkov, E. Semenova, Materials Science International Team, MSIT®, Fe-Li Binary Phase Diagram Evaluation \Textperiodcentered Phase diagrams, Crystallographic and Thermodynamic data: Datasheet from MSI Eureka in SpringerMaterials, MSI Materials Science International Services GmbH, https://materials.springer.com/msi/docs/sm_msi_r_20_018967_01.
[24] F.A. Hernández, F. Arbeiter, L.V. Boccaccini, E. Bubelis, V.P. Chakin, I. Cristescu, B.E. Ghidersa, M. González, W. Hering, T. Hernández, X.Z. Jin, M. Kamlah, B. Kiss, R. Knitter, M.H.H. Kolb, P. Kurinskiy, O. Leys, I.A. Maione, M. Moscardini, G. Nádasi, H. Neuberger, P. Pereslavtsev, S. Pupeschi, R. Rolli, S. Ruck, G.A. Spagnuolo, P.V. Vladimirov, C. Zeile, G. Zhou, Overview of the HCPB research activities in EUROfusion, IEEE Trans. Plasma Sci. 46 (2018) 2247–2261, doi:10.1109/TPS.2018.2830813.
[25] T. Hernández, A. Moroño, F.J. Sánchez, C. Maffiotte, M.A. Monclús, R. González-Arrabal, Study of deuterium permeation, retention, and desorption in SiC coatings submitted to relevant conditions for breeder blanket applications: thermal cycling effect under electron irradiation and oxygen exposure, J. Nucl. Mater. 557 (2021) 153219, doi:10.1016/j.jnucmat.2021.153219.
[26] T. Hernández, F.J. Sánchez, F. Di Fonzo, M. Vanazzi, M. Panizo, R. González-Arrabal, Corrosion protective action of different coatings for the helium cooled pebble bed breeder concept, J. Nucl. Mater. 516 (2019) 160–168, doi:10.1016/j.jnucmat.2019.01.009.
[27] T. Hernández, F.J. Sánchez, A. Moroño, E. León-Gutiérrez, M. Panizo-Laiz, M.A. Monclus, R. González-Arrabal, Corrosion behavior of diverse sputtered coatings for the helium cooled pebbles bed (HCPB) breeder concept, Nucl. Materi. Energy 25 (2020) 100795, doi:10.1016/j.nme.2020.100795.